J Sol-Gel Sci Technol (2011) 60:137–143
DOI 10.1007/s10971-011-2569-6

ORIGINAL PAPER

Enhancement of fluorescence and lasing properties of covalent bridged fluorescent dye in organic–inorganic hybrid materials

Seung-Yeon Kwak · Na Ree Kim · Kangin Lee · Jonghoon Yi · Jae Hong Kim · Byeong-Soo Bae

Received: 25 March 2011 / Accepted: 16 August 2011 / Published online: 31 August 2011

Abstract Fluorescent dye (DCM-OH) is covalently bridged to organic–inorganic hybrid material to prevent molecular stacking and to get high fluorescence efficiency and laser property. Novel DCM-OH is synthesized to have hydroxyl functional groups and is bridged to trialkoxysilane as a sol–gel precursor. It participates in sol–gel process to synthesize dye-bridged organic–inorganic hybrid material (dye-bridged hybrimer) and solid-state dye laser sample is ready through polymerization. Fluorescence property of dye-bridged hybrimer is compared with DCM-doped hybrimer that is simple mixture of DCM-OH and hybrimer matrix. The covalently bridged structure of hybrimer with DCM-OH prevented the stacking of fluorescent molecules and enhanced concentration stability. The dye-bridged hybrimer shows much higher fluorescence intensity and low color-shift until it reached high concentration in comparison with DCM-doped system. And the proper lasing property is observed in dye-bridged hybrimer samples.

S.-Y. Kwak · N. R. Kim · B.-S. Bae (✉)
Department of Materials Science and Engineering, Laboratory of Optical Materials and Coating (LOMC), Korea Advanced Institute of Science and Technology (KAIST), Daejeon 305-701, Korea
e-mail: bsbae@kaist.ac.kr

N. R. Kim · J. H. Kim (✉)
Department of Display and Chemical Engineering, Yeungnam University, Gyeongsan 712-749, Korea
e-mail: jaehkim@ynu.ac.kr

K. Lee · J. Yi
Department of Physics, Yeungnam University, Gyeongsan 712-749, Korea

Keywords Solid-state dye laser · Organic–inorganic hybrid material · Covalently bridged fluorescent dye · Sol–gel process

1 Introduction

Dye laser systems offer crucial advantages such as high quantum efficiency, a large choice of pump sources and broad emission bands, when used as lasers and as optically pumped amplifiers [1]. While dye lasers based on solid-state matrices provide further advantages over liquid systems, such as compact and inexpensive manufacturing processes, short maintenance times and non-toxic, non-volatile, non-flammable media, their use however currently remains rather limited in practical applications [2–4]. An intensive effort has been made to develop solid-state dye laser devices with high optical quality, high thermal conductivity and high laser damage thresholds, thus providing the necessary properties for practical, high performance dye laser devices [5–8].

Several kinds of solid-state matrices, including PMMA, polymer-glass composite, cholesteric polymer networks, organically modified silicate (ormosil) glass and sol–gel glass have been investigated as host media for solid-state dye lasers [9–14]. Organic matrices have low fabrication costs and are simple to prepare; however they have inherently poor thermo-mechanical and photo-stability properties. On the other hand, inorganic matrices such as sol–gel derived silica and zirconia show enhanced stability and efficiency and include good transmission behavior in the UV–Vis region [15–18]. Nevertheless, in many cases they are not suitable for solid-state dye lasers since they require elevated temperatures during the manufacturing process.

Recently we have reported that sol–gel process-based organic–inorganic hybrid materials (hybrimers) are suitable for optical matrix production [19, 20]. These hybrimers combine the characteristic advantages of both organic polymer and inorganic matrices, including the good thermal, mechanical, and optical properties of transparent inorganic glasses. They can be applied to the fabrication of cheap and robust matrix, like organic polymers, they can be solution processed and polymerized at lower temperatures. It is also easy to control the material properties of these hybrimers through the selection of suitable precursors and optimized processing parameters. When combined, these properties mean that hybrimers are an enticing candidate as the host matrices of solid-state dye lasers.

Fluorescent dye molecules have large π-conjugated planar structures which would induce strong molecular stacking in the solid-state and result in poor solubility with dye laser process media. It is well known that molecular stacking of fluorescence materials significantly reduces the fluorescence intensity; therefore a dye concentration of less than 1×10^{-3} mol/L is generally used in existing dye laser devices [21]. Dendrimer, non-aqueous sol–gel material and dye hybrid silica have all been used to overcome this molecular stacking problem and improve the fluorescence properties of these materials [22–25].

In this study, a dye-bridged methacrylate hybrimer was prepared, being covalently bridged with DCM-OH consisted of (2,6-dimethyl-4H-pyran-4-ylidene)malononitrile, with the aim of enhancing the lasing performance by improving the mixability and dispersion in the matrix. This was compared with the DCM-doped methacrylate hybrimer which is mixture of DCM-OH and hybrimer matrix. We prepared the hydroxyl functional DCM (DCM-OH) that can easily react with a silane precursor. The precursor then produces dye-grafted alkoxysilane, ready for bonding with the hybrimer matrix. This was used in a sol–gel process to synthesize dye-bridged oligosiloxane resin which was then cured by methacrylate polymerization to fabricate the dye-bridged hybrimer.

2 Experimental section

2.1 Synthesis of hydroxyl-functional DCM (DCM-OH)

Both 4-diethylamino-2-(6-hydroxy-hexyloxy)-benzaldehyde (16.47 mmol) and (2,6-dimethyl-4H-pyran-4-ylidene)malononitrile (6.1 mmol) were dissolved in 30 mL of dry acetonitrile in the presence of piperidine (6.1 mmol). The reaction mixture was then refluxed for 3 h. Fifteen millilitre of methanol was added after cooling the solution to room temperature in order to precipitate the crude product from the reaction solution. This precipitate appeared as a reddish powder. The final product was obtained by washing the precipitate with MeOH/$CHCl_3$ (4/1) 3 times, leaving a dark red powder. ^{1}H NMR (300 MHz, $CDCl_3$): 7.69–7.63 (d, 2H), 7.32–7.29 (d, 2H), 6.84–6.79 (d, 2H), 6.45 (s, 1H), 6.31–6.28 (d, 2H), 6.13 (s, 2H), 4.09–4.05 (t, 4H), 3.61–3.56 (q, 4H), 3.45–3.36 (q, 8H), 1.95–1.82 (m, 8H), 1.56–1.46 (m, 12H), 1.24–1.08 (t, 12H).

2.2 Synthesis of dye-bridged methacrylate oligosiloxane

To facilitate chemical bonding of the DCM-OH with oligosiloxane, dye-grafted alkoxysilane was first synthesized. The above-mentioned DCM-OH was used as a precursor with 3-(triethoxysilyl)propyl isocyanate (ICPTES), mixed in a 1:2 molar ratio. The mixture was stirred for 3 h at 80 °C to promote a urethane reaction between the isocyanate group in ICPTES and the hydroxyl group of DCM-OH, resulting in the synthesis of dye-grafted alkoxysilane. This reaction was occurred in the closed flask. The dye-bridged oligosiloxane was then synthesized by reacting the prepared dye-grafted alkoxysilane, 3-(trimethoxysilyl)propyl methacrylate (MPTS, 0.068 mol) and diphenylsilanediol (DPSD, 0.068 mol) via a sol–gel process. This involved mixing and stirring the dye-grafted alkoxysilane and MPTS for 1 h with barium hydroxide monohydrate, which was used as a catalyst. During this process the DPSD was continuously added to the mixture solution to prevent self-condensation, and the amount of DPSD was fixed at 50 mol% of the total precursors. The mixture was then reacted for 12 h at 80 °C to complete the formation of siloxane networks. DPSD has merit on forming siloxane bonds in this sol–gel process because silanol groups contained in DPSD start to react with alkoxy groups in organo alkoxysilanes under low temperature [26]. The siloxane bonds are formed between dimeric (D) species Si of DPSD and trimeric (T) species Si of organo alkoxysilanes. The byproduct, alcohol, was removed by nitrogen purging during this reaction. Finally, we could obtain dye-bridged oligosiloxane. The DCM-OH concentration was controlled between 1×10^{-4} mol/L and 6.5×10^{-3} mol/L in the synthesized dye-bridged oligosiloxane. DCM-doped oligosiloxane was prepared separately for comparison, involving the production of methacrylate oligosiloxane resin, synthesized by the same sol–gel reaction of MPTS and DPSD but without adding the dye-grafted alkoxysilane. Otherwise the composition and synthesis procedure was same as for the dye-bridged oligosiloxane. DCM-OH was then dissolved in chloroform and mixed uniformly with this methacrylate oligosiloxane resin and the solvent was removed by vacuum evaporation from the flask. The molecular design and synthesis scheme of the dye-bridged oligosiloxane are shown in Scheme 1.

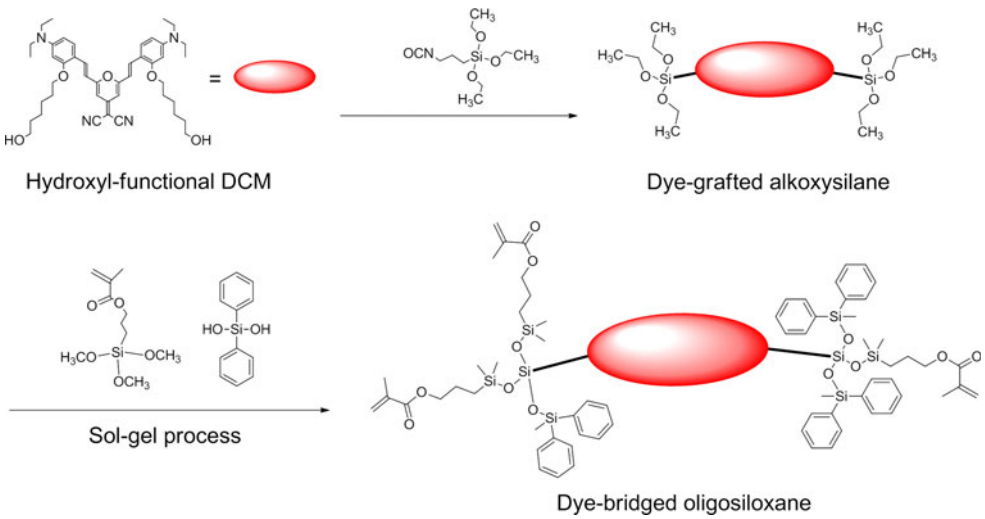

Scheme 1 Synthesis scheme of dye-grafted alkoxysilane and dye-bridged hybrimer via sol–gel process

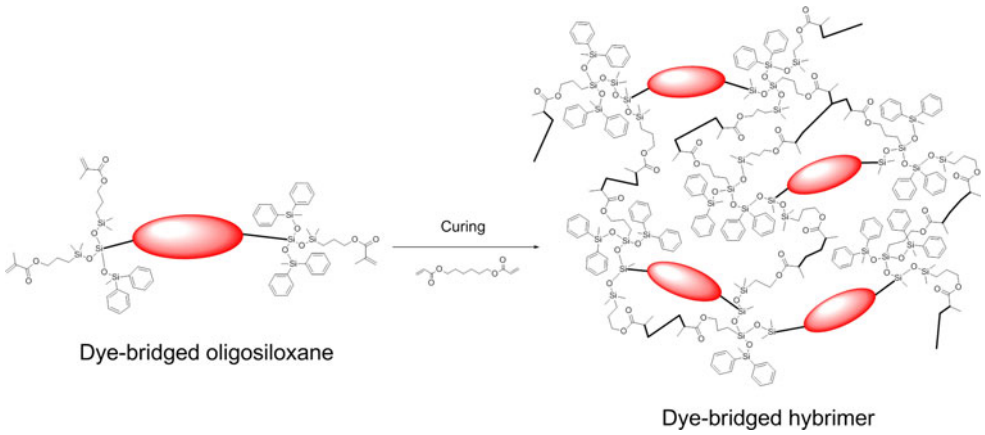

Scheme 2 Schematic structure dye-bridged hybrimer after curing dye-bridged methacrylate oligosiloxane

2.3 Fabrication of dye-bridged hybrimer for solid-state dye laser

To prepare the dye-bridged hybrimer, the synthesized dye-bridged oligosiloxane resin was mixed with 1,6-Hexanediol diacrylate (HDDA), with an equivalent molar ratio of 1:0.6, as a cross-linker and 2 wt% of dicumyl peroxide as a catalyst of thermal curing. The mixture was then poured into a prepared polydimethylsiloxane (PDMS) mold to form a bulk sample and polymerized at 120 °C for 1 h. The shrinkage is rarely occurred. The resulting fabricated dye-bridged hybrimer, for fluorescence and lasing property measurements, had a size of 10 mm diameter and 5 mm thickness. The sample surface quality was transformed to an optical grade after a series of polishing processes. DCM-doped hybrimer was fabricated with the above dye-bridged hybrimer procedure, while using DCM-doped oligosiloxane. Scheme 2 shows a schematic structure of the dye-bridged hybrimer.

2.4 Fabrication of a waveguide pattern in dye-bridged hybrimer

We followed the thermowetting embossing imprinting technique [27] to fabricate a waveguide pattern in the dye-bridged hybrimer. A master structure was first fabricated on a silicon wafer using standard electron beam lithography. An elastomeric stamp of the master structure was prepared using PDMS to create a mold replica. The dye-bridged oligosiloxane was mixed with photoinitiator (2,2-dimethoxy-2-phenylacetophenone), dispersed on the bare Si wafer and heated to 80 °C to ensure wetting around the structuring area. The elastomeric stamp was placed onto the dispersed dye-bridged oligosiloxane, ensuring complete coverage from edge to edge along the line pattern and preventing vapors from trapping. The dye-bridged oligosiloxane covered with the stamp was photo cured using a UV lamp, meaning fabrication of a waveguide structure was completed within two minutes. After

detaching the elastomeric stamp the micron line pattern of dye-bridged hybrimer was obtained.

2.5 Characterization

Fourier transform infrared (FT-IR) spectra of the oligosiloxane resin were recorded using an FT-IR spectrometer (Jasco, 680plus) with 4 cm^{-1} scanning resolution in the 650–4,000 cm^{-1} wavenumber range. Fluorescence characteristics were measured with photoluminescence spectroscopy (PSI Korea, DARSA PRO 5100) using a Xe lamp as an excitation source, at room temperature. For the measurement of lasing properties and amplified spontaneous emission (ASE) of this fluorescence material system, the solid-state dye laser sample was placed on an optical mount. As a pumping laser we used the second harmonic beam (532 nm) of a flash lamp pumped Nd:YAG laser (Quantel, YG980E−10). The second harmonic beam provided maximum pulse energy of 150 mJ, with a full width at half maximum (FWHM) pulse width of 10 ns and pulse repetition rate of 10 Hz. A cylindrical lens with 10 cm focal length was used to focus the pump beam on the dye surface. Measured at the dye cell surface, the line shaped pump beam was 8 mm in width across the optical axis (horizontal axis parallel to the optical table) and 0.1 mm high in the vertical direction. The lasing property was measured after assembling a simple 5 cm linear cavity. The end mirror had reflectance of 99% over the 550–750 nm range. Various output couplers, with reflectivities of 30, 50, 70, and 90%, over the same range, were used to find the reflectivity combination which produces the highest conversion efficiency. The pulse energy of both the dye laser and pump laser were calculated by measuring average powers with a laser power meter (Ophir, Nova 1) and converting them into pulse energies, taking into account the pulse repetition rate. The pulse width of the dye laser output was also measured using a fast silicon photodiode (Thorlab, DET 210). Finally, the fabricated waveguide pattern was observed with an optical microscope (Nikon, Eclipse L150).

3 Results and discussion

3.1 Bonding structure analysis of dye-bridged methacrylate oligosiloxane

The DCM-OH was covalently bridged to alkoxysilane through urethane bonding between the ICPTES and DCM-OH, producing chemically stable structures. FT-IR analysis provides specific information about the bonding structure, as shown in Fig. 1a. FT-IR spectra of before and after reactions are normalized using the silicon alkoxide band at

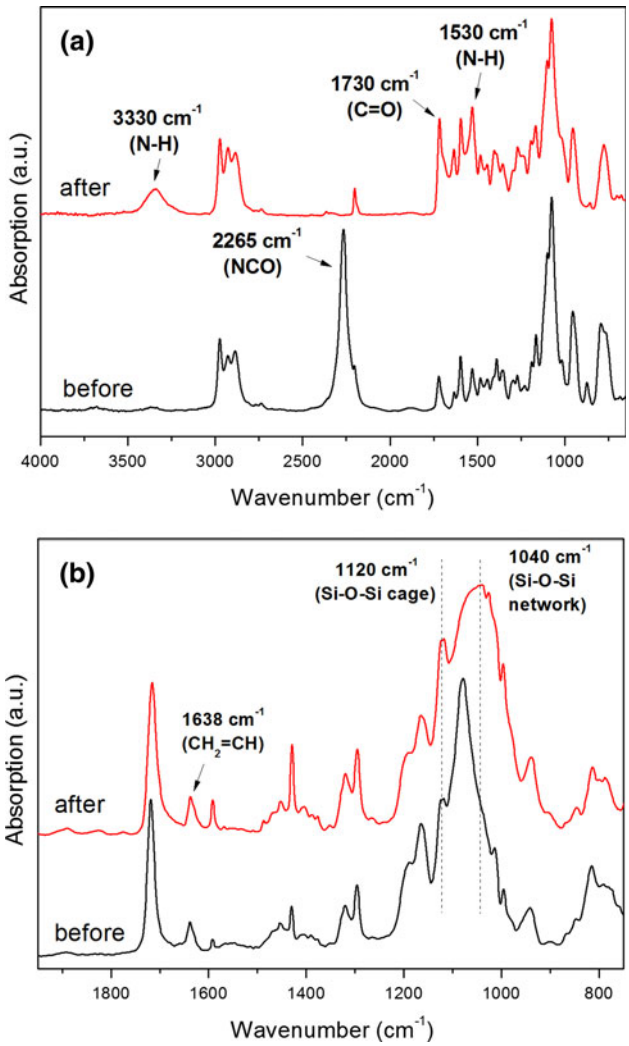

Fig. 1 **a** FT-IR spectra of the precursor mixture of DCM-OH and ICPTES before and after reaction for synthesis of dye-grafted alkoxysilane. **b** FT-IR spectra of the dye-bridged methacrylate oligosiloxane

1,080 cm^{-1} and C–H stretching band at 2,800–3,000 cm^{-1}, because they are not related to the urethane formation. After the ICPTES and DCM-OH are mixed, an isocyanate double band peak is clearly observed at 2,265 cm^{-1}. After reaction at 80 °C for 3 h this isocyanate double band peak is seen to have disappeared, indicating that the isocyanate is completely consumed during the chemical reaction. A small band at 2,200 cm^{-1} is caused by carbon dioxide and can be considered as experimental noise. A new band of urethane related bonds is found at 3,330 cm^{-1} being the N–H stretching band of urethane groups, along with intensity increases around 1,730–1,530 cm^{-1} which assign to the 1,730 cm^{-1} band of urethane C=O groups and the 1,530 cm^{-1} band of N–H [28]. It can thus be concluded that ICPTES and DCM-OH are covalently bridged and the dye-grafted alkoxysilane is successfully synthesized.

Using precursors including dye-grafted alkoxysilane, MPTS and DPSD, dye-bridged methacrylate oligosiloxane was synthesized via the described sol–gel reaction and its FT-IR spectra are shown in Fig. 1b. The absorption band of CH_2=CH resulting from the appearance of methacryl groups can be seen at 1,638 cm^{-1}. The peak position and intensity of this methacryl band are rarely changed before and after reaction which means unwanted methacryl breakage is not occurred during sol–gel reaction. As the sol–gel reaction continues, two types of siloxane bond (Si–O-Si) appear in the range of 1,000–1,150 cm^{-1}. The Si–O-Si cage structure peak at 1,120 cm^{-1} and the Si–O-Si network structure peak at 1,040 cm^{-1} appear after the completed reaction. The silicon alkoxide band at 1,080 cm^{-1} is seen to decrease as silicon alkoxides in the MPTS and ICPTES change to siloxane bonds. The siloxane band shown in FT-IR spectra was gradually increased during reaction and the complete formation of siloxane bond was achieved after 12 h at 80 °C. FT-IR spectra of siloxane band were not changed after 12 h reaction which means siloxane bonding is complete in this system. These siloxane structures affect the mechanical, thermal and optical properties of the resulting material. It should be noted that the solid-state dye laser sample showed shrinkage and cracks when siloxane bonding in the dye-bridged hybrimer was incomplete. Unreacted monomers which do not participate in forming oligosiloxane and low molecular species may cause the shrinkage and cracks during fabrication of the solid-state dye laser sample. Using completely reacted dye-bridged hybrimer with highly dense siloxane, mechanical and thermal stabilities were achieved.

3.2 Fluorescence properties of dye-bridged hybrimer

Although the fluorescence efficiency of laser dye is high at high concentrations, as the concentration is increased this efficiency diminishes at a certain concentration due to molecular stacking. Figure 2a represents fluorescence spectra from a dye-bridged hybrimer with DCM-OH concentration of 1×10^{-3} mol/L (curve i) and DCM-doped hybrimers with 1×10^{-3} mol/L (curve ii) and 3×10^{-3} mol/L (curve iii). The samples fluoresce with peak maxima at 635 nm for the DCM-doped hybrimer and 616 nm from the dye-bridged hybrimer at the same concentrations of 1×10^{-3} mol/L. This bathochromic shift which represents J-aggregate is caused by self-absorption by the aggregated DCM-OH molecules in the DCM-doped hybrimer. Additionally, in the DCM-doped hybrimer case, when the DCM-OH concentration was higher than 1×10^{-3} mol/L, the fluorescence main peak is separated into two peaks, at 600 and above 660 nm, as shown in curve iii of Fig. 2a. These peaks represent re-absorption and re-emission phenomena between monomers and dimers caused by DCM-OH molecules stacking in the matrix. In contrast, the dye-bridged hybrimer maximum peak shift was within 10 nm until the DCM-OH concentration increases 65 times from 1.0×10^{-4} mol/L to 6.5×10^{-3} mol/L and the broad emission shape of fluorescence peak is also maintained.

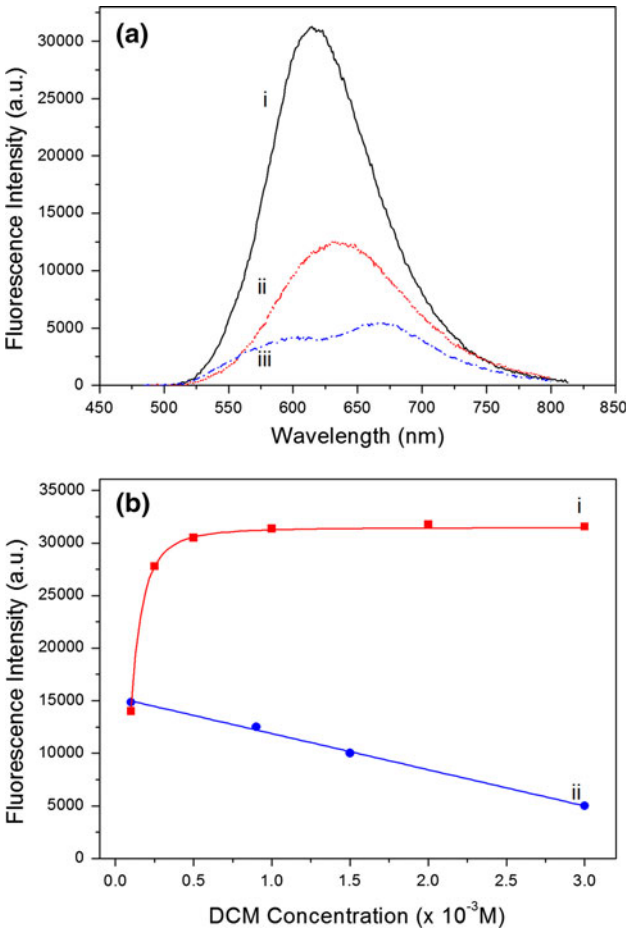

Fig. 2 **a** Fluorescence spectra of dye-bridged hybrimer with DCM-OH concentration of 1×10^{-3} mol/L (*curve* i) and DCM-doped hybrimer with 1×10^{-3} mol/L (*curve* ii) and DCM-doped hybrimer with 3×10^{-3} mol/L (*curve* iii). **b** Dependence of fluorescence intensity on the DCM-OH concentration of dye-bridged hybrimer (*curve* i) and DCM-doped hybrimer (*curve* ii)

The dependence of fluorescence intensity on the DCM-OH concentration of both the dye-bridged hybrimer and the DCM-doped hybrimer are also shown in Fig. 2b. For the low DCM-OH concentration ($\sim 1 \times 10^{-4}$ mol/L) case, the fluorescence intensities from both samples are almost identical. As the concentration is increased the fluorescence intensity of the DCM-doped hybrimer decreases significantly. However the fluorescence intensity from the dye-bridged hybrimer is not seen to reduce until the DCM-OH concentration reaches 3×10^{-3} mol/L. At this concentration the fluorescence intensity of the dye-bridged hybrimer was 6 times higher than that of the DCM-doped hybrimer. The difference in color-shift and fluorescence intensities of

the two samples indicates that the covalently bridged structure effectively prevents DCM-OH stacking-induced fluorescence quenching. When each DCM-OH molecule is covalently bridged to the bulky hybrimer matrix, DCM-OH aggregation can be avoided up to higher DCM-OH concentrations, conserving high fluorescence efficiencies.

3.3 Lasing properties of dye-bridged hybrimer

Solid-state hybrimer dye laser samples, with different DCM-OH concentrations, were prepared for lasing property measurements. Laser emission was observed in samples with DCM concentrations from 5×10^{-4} mol/L to 4×10^{-3} mol/L. The highest emission output was produced in the samples with DCM-OH concentration in the range of 1×10^{-3} mol/L to 3×10^{-3} mol/L. Figure 3 shows the spectral profiles of the stimulated dye laser emission and amplified spontaneous emission (ASE) from the dye-bridged hybrimer samples. Although the main absorption in the dye-bridged hybrimer is around 460 nm, laser emission was successful using a 532 nm pumping source (second harmonic beam of Nd:YAG laser) because the dye-bridged hybrimer has a broad absorption band. The ASE curve indicates that the dye-bridged hybrimer has a tunable wavelength range of 200 nm (550–750 nm). The laser emission peaks appear at 627 nm with the full width half maximum (FWHM) of 6 nm. The laser emission spectra are much narrower than those of the fluorescence due to the stimulated emission. In comparison to the dye-bridged hybrimer, the DCM-doped hybrimer sample shows no lasing property at any DCM-OH concentration over 1.0×10^{-4} mol/L. This is due to the extremely low

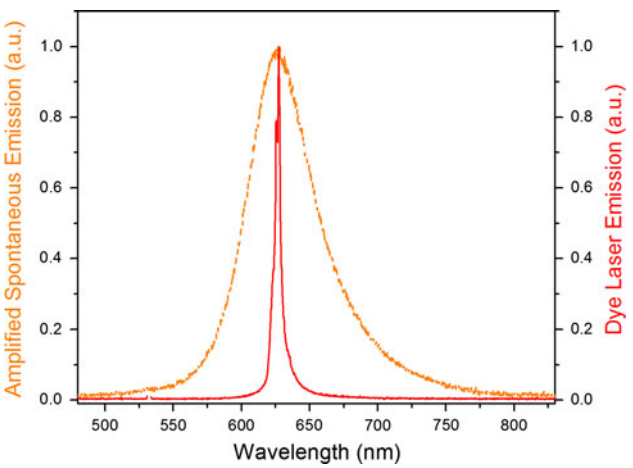

Fig. 3 Spectral profiles of the stimulated dye laser emission (*solid line*) and amplified spontaneous emission spectrum (*dotted line*) of the dye-bridged hybrimer when pumping source is Nd:YAG laser (532 nm)

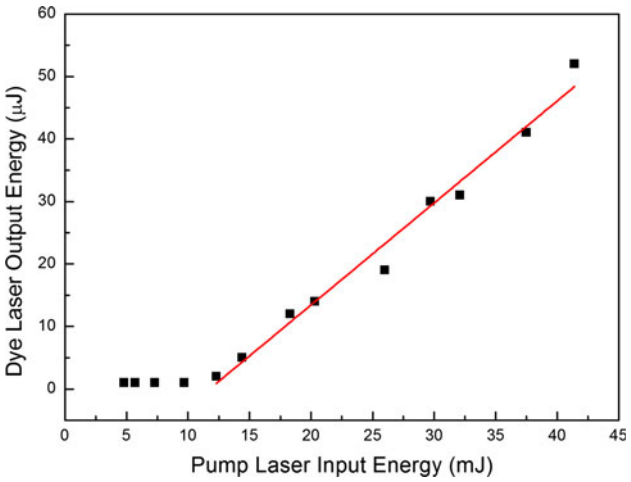

Fig. 4 Output emission energy of solid-state hybrimer dye laser as a function of input energy of pump laser

stimulation efficiency caused by dye aggregation. Figure 4 represents the output emission energy of the dye-bridged hybrimer as a function of input energy of the pump laser. Lasing starts when the pump laser energy is 4 mJ and the lasing threshold is 11.7 mJ. The maximum output laser energy is acquired with the pump laser at 41 mJ with a slope efficiency of 0.16%. The hybrimer sample is seen to be thermally stable and undamaged by pump laser energy up to 50 mJ. So we can conclude that the dye-bridged system offers proper laser property in comparison to the simple mixture of dye and matrix.

3.4 Dye-bridged hybrimer-waveguide patterning

The dye-bridged hybrimer can be patterned to fabricate a channel waveguide for waveguide laser applications, via a simple imprinting process. Due to its geometry, the channel waveguide laser architecture has many advantages over bulk lasers. Beam divergence is restricted as the beam is confined in the waveguide. This result in high optical gains with low threshold powers and the optical intensity can be preserved over a longer distance. Also, it can be used in integrated optoelectronic device applications [29–31]. In this study the micron-sized waveguide pattern was fabricated with a thermowetting embossing process. Figure 5 shows an optical microscope image of the waveguide patterned in the dye-bridged hybrimer film. The image was taken under the illumination of a 365 nm UV lamp. The width and thickness of the waveguide pattern are 40 and 20 μm, respectively. The gap between each waveguide pattern is 200 μm. Uniform reddish fluorescence can be observed along the waveguide pattern. This result shows that dye-bridged hybrimer patterning can provide a facile method for the fabrication of solid-state waveguide lasers.

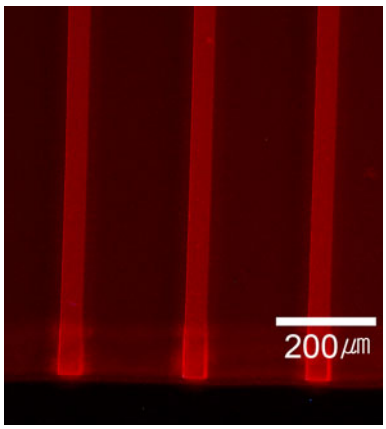

Fig. 5 Optical microscope image of waveguide pattern consisted of dye-bridged hybrimer under illumination of UV lamp. The width of the waveguide pattern is 40 μm and the gap between patterns is 200 μm

4 Conclusion

The covalently bridged DCM had been fabricated within a sol–gel based organic–inorganic hybrid network structure. Its fluorescence properties and lasing emission characters were measured and compared with that of the DCM-doped system which revealed that the dye-bridged hybrimer showed superior fluorescence characteristics. As the dye concentration is increased, the intensity of fluorescence of the DCM-doped hybrimer quenched significantly due to the molecular stacking in the solid state, however, the dye-bridged hybrimer exhibited continuous increasing fluorescence intensity and its main absorption peak is less shifted until the dye concentration reaches a relatively high level. We conclude that molecular stacking is prevented by the covalently bridged structure of the dye-bridged hybrimer with the organic–inorganic network, where each dye molecule is seized by alkoxysilane and is caged in the siloxane network. Using the dye-bridged hybrimer a solid-state dye laser was fabricated, with lasing emission observed at 627 nm and a FWHM of 6 nm. The dye-bridged hybrimer also shows potential for easy fabrication in solid-state waveguide laser design. We believe that practically useful solid-state dye laser devices can be achieved by exploiting the design of fluorescence materials and their aggregation control for material system.

Acknowledgments This research was supported by Basic Science Research Program through the National Research Foundation of Korea (NRF) funded by the Ministry of Education, Science and Technology (R01-2007-000-20815-0 (2009)).

References

1. Dubois A, Canva M, Brun A, Chaput F, Boilot J-P (1996) Appl Opt 35:3193
2. Hermes RE, Allik TH, Chandra S, Hutchinson JA (1993) Appl Phys Lett 63:877
3. Nhung TH, Canva M, Dao TTA, Chaput F, Brun A, Hung ND, Boilot J-P (2003) Appl Opt 42:2213
4. Lam KS, Lo D (1998) Appl Phys B 66:427
5. Bergmann A, Holzer W, Stark R, Gratz H, Penzkofer A, Amat-Guerri F, Costela A, Garcia-marieno I, Sastre R (2001) Chem Phys 271:201
6. Faloss M, Canva M, Georges P, Brun A, Chaput F, Boilot J-P (1997) Appl Opt 36:6760
7. Lin HT, Bescher E, Mackenzie JD, Dai H, Stafsudd OM (1992) J Mater Sci 27:5523
8. Costela A, Garcia-marieno I, Barroso J, Sastre R (1998) J Appl Phys 83:650
9. Cazeca MJ, Jiang X, Kumar J, Tripathy SK (1997) Appl Opt 36:4965
10. Suratwala T, Gardlund Z, Davidson K, Uhlmann DR (1997) J Sol-Gel Sci Technol 8:953
11. Rahn MD, King TA (1998) J Mod Opt 45:1259
12. He GS, Bhawalkar JD, Zhao CF, Park CK, Prasad PN (1996) Appl Phys Lett 68:3549
13. Schmidtke J, Stille W, Finkelmann H, Kim ST (2002) Adv Mater 14:746
14. Yagi K, Shibata S, Yano T, Yasumori A, Yamane M, Dunn B (1995) J Sol-Gel Sci and Tech 4:67
15. Canva M, Georges P, Perelgritz J-F, Brum A, Chaput F, Boilot J-P (1995) Appl Opt 34:428
16. Knobbe ET, Dunn B, Fuqua PD, Nishida F (1990) Appl Opt 29:2729
17. Yariv E, Reisfeld R (1999) Opt Mater 13:49
18. Zhu X-L, Lo D (2000) Appl Phys Lett 77:2647
19. Kang DJ, Bae BS (2007) Acc Chem Res 40:903
20. Kang DJ, Kim WS, Bae BS (2005) Appl Phys Lett 87:22106/1
21. Yokoyama S, Nakahama T, Mashiko S (2005) J Lumin 111:285
22. Yokoyama S, Otomo A, Mashiko S (2002) Appl Phys Lett 80:7
23. Menaa B, Takahashi M, Tokuda Y, Yoko T (2008) J Photochem Photobiol A 194:362
24. Carbonaro CM, Anedda A, Grandi S, Magistris A (2006) J Phys Chem B 110:12932
25. Cui Y, Yu J, Gao J, Wang Z, Qian G (2009) J Sol-Gel Sci Technol 52:362
26. Eo YJ, Lee TH, Kim SY, Kang JK, Han YS, Bae BS (2005) J Polym Sci Pol Phys 43:827
27. Kim WS, Kim KS, Kim YC, Bae BS (2005) Thin Solid Films 476:181
28. Lobo H, Bonilla JV (2003) Handbook of plastics analysis. Crc Press
29. Hanna DC, Large AC, Shepherd DP, Tropper AC, Chartier I, Ferrand B, Pelenc D (1993) Appl Phys Lett 63:7
30. Yang P, Wirnsberger G, Huang HC, Cordero SR, McGehee MD, Scott B, Deng T, Whitesides GM, Chmelka BF, Buratto SK, Stucky GD (2000) Science 287:465
31. Mackenzie JI (2007) IEEE J Sel Top Quantum Electron 13:626